Paper submitted for publication in Water Research

Interactions of dissolved humic substances with oppositely charged fluorescent dyes for tracer techniques

Akira Hafuka [a,*], Qing Ding [b], Hiroshi Yamamura [a], Koji Yamada [c], Hisashi Satoh [d]

[a] Department of Integrated Science and Engineering for Sustainable Society, Faculty of Science and Engineering, Chuo University, 1-13-27 Kasuga, Bunkyo-ku, Tokyo 112-8551, Japan

[b] Division of Civil and Environmental Engineering, Graduate School of Science and Engineering, Chuo University, 1-13-27 Kasuga, Bunkyo-ku, Tokyo 112-8551, Japan

[c] Division of Environmental Materials Science, Graduate School of Environmental Science, Hokkaido University, North-10, West-5, Sapporo 060-0810, Japan

[d] Division of Environmental Engineering, Graduate School of Engineering, Hokkaido University, North-13, West-8, Sapporo 060-8628, Japan

E-mail address:

Akira Hafuka: hafuka.14p@g.chuo-u.ac.jp

Qing Ding: dingqing1988@gmail.com

Hiroshi Yamamura: yamamura.10x@g.chuo-u.ac.jp

Koji Yamada: yamada@ees.hokudai.ac.jp

Hisashi Satoh: qsatoh@eng.hokudai.ac.jp

* *Corresponding author.* Akira Hafuka

Tel. & fax: +81-3-3817-7283

E-mail: hafuka.14p@g.chuo-u.ac.jp

Abstract

To investigate interactions between oppositely charged fluorescent dyes and dissolved humic substances, fluorescence quenching of fluorescein and rhodamine 6G with dissolved humic substances was performed. Binding coefficients were obtained by the Stern–Volmer equation. The fluorescence of rhodamine 6G was largely quenched by the addition of humic acid and a non-linear Stern–Volmer plot was obtained. This strong quenching may be caused by the electrostatic interaction between cationic rhodamine 6G and humic acid and strengthened by the hydrophobic repulsion. In contrast, the quenching and interactive effects of dissolved humic substances for fluorescein were relatively weak.

Keywords: Tracer, Stern–Volmer plot, Fluorescein, Rhodamine 6G

1. Introduction

Fluorescent dyes have been widely employed in various technologies such as dye tracing, bio-imaging, chemical sensing, and dye lasers (Yuan et al., 2013;

Basabe-Desmonts et al., 2007; Li and Psaltis, 2008; Harden et al., 2008). Dye tracer techniques are powerful tools that enable better understanding of solute transport in the liquid phase under a variety of hydrological conditions by tracking natural tracers and/or spiked artificial tracers. In the field of water and environmental engineering, tracers have been applied to investigate water flow in surface and ground water systems, as well as in laboratory experiments (Goppert and Goldscheider, 2008; Jones and Smith, 2005; Sabaliunas et al., 2003). To be effective, tracers must be absent from (or present in very low concentrations) natural aquatic environments, have high water solubility and low sorptiivity to soil and sediment, be safe, highly detectable, and chemically, physically, and biologically stable. Among a variety of tracers, fluorescent dyes composed of synthetic organic compounds possess most of these characteristics, are cost effective and easy to use, and can be easily identified on-site using a portable fluorometer. Fluorescein is a popular fluorescent dye tracer commonly used in aquatic systems (Sabaliunas et al., 2003; Harden et al., 2008). Rhodamine 6G is also sometimes used as a fluorescent dye tracer (Kwak et al., 2013); however, this compound has been shown to have toxic effects and is therefore generally limited to use in laboratory experiments (Alford et al., 2009). The difference of two dyes is that fluorescein is anionic and rhodamine 6G is cationic.

Smart and Laidlaw (1977) investigated the sensitivity, detectability, effect of water chemistry, decay rates, adsorption resistance, toxicity, and cost of eight fluorescent dye tracers, including fluorescein. Since then, ecotoxicological assessments (Behrens et al., 2001), photobleaching (Larsen and Crimaldi, 2006), and effects of solvents and pH (Saini et al., 2009; Oba and Poulson, 2012) of fluorescent dye tracers have been investigated. However, no studies have focused on the effects of dissolved humic substances (DHS) on fluorescent dyes. Although fluorescent dyes can be used for qualitative analysis, the interactions might inhibit the optical detection of fluorescent dyes due to the potential quenching caused by the presence of DHS. DHS is known to interact with organic compounds such as herbicides, pesticides, and polycyclic aromatic hydrocarbons (PAHs) in surface water (Ravacha and Rebhun, 1992; Schlautman and Morgan, 1993; Hesketh et al., 1996; Spark and Swift, 2002), and to affect their fate and transport. Various methods such as simple adsorption experiments, dialysis, microcalorimetry, reverse phase separation, solubility enhancement, and fluorescence quenching have been used to investigate the interactions between DHS and these organic compounds (Hesketh et al., 1996; Spark and Swift, 2002; Raber et al., 1998; Yamamoto et al., 2003; Schlautman and Morgan, 1993). Fluorescence quenching is a

simple and useful method commonly employed to investigate interactions of DHS with PAHs because some PAHs show fluorescence and DHS acts as a quencher. The Stern–Volmer equation (also known as the fluorescence static quenching equation) can be plotted by conducting fluorescence quenching experiments (Gauthier et al., 1986). The binding coefficient can be obtained easily by determining the slope of the Stern–Volmer plot. In this study, the fluorescence quenching method was applied to analyze interactions of oppositely charged fluorescent dyes, fluorescein and rhodamine 6G, with DHS to investigate its effects on the dyes. This paper would contribute to the practice of selecting suitable fluorescent dye tracers in aquatic and hydrology studies.

2. Materials and methods

2.1 Fluorescent dyes

The chemical structures of fluorescein, rhodamine 6G, and rhodamine B are shown in Fig. 1. All fluorescent dyes are xanthene derivatives with many valuable characteristics, including sharp and intense absorption and fluorescence bands, high fluorescence quantum yields, high molar absorption coefficients, good photo-chemical stability,

relatively long emission wavelength, and good water solubility (Chen et al., 2012). Fluorescein sodium salt (MW: 376.27), rhodamine 6G (MW: 479.01), and rhodamine B (MW: 479.01) were purchased from Sigma-Aldrich (St. Louis, United States) and used without further purification.

2.2 Sample preparation and fluorescence quenching experiments

Fluorescence quenching experiments were conducted in batch experiments. Stock solutions of the fluorescent dyes (330 μM) were prepared by dissolving the dyes separately in Milli-Q water (18.25 MΩcm). IHSS Suwannee River Humic Acid Standard II (2S101H) and Fulvic Acid Standard II (2S101F) were used as humic substances standards. The humic substances were dissolved in Milli-Q water, filtered through a 0.45-μm-pore-size membrane (A045A047A; Toyo Roshi Kaisya, Ltd., Tokyo, Japan) and stored separately as DHS stock solutions. Dissolved organic carbon (DOC) concentrations of the stock solutions were determined using a total organic carbon analyzer (TOC-L CSH; Shimadzu Corporation, Kyoto, Japan). Test solutions were prepared by adding 30 μL of the dye stock solution and an appropriate volume of the DHS stock solution into 200 μL of sodium phosphate buffer (10 mM, pH 6.9) in a

10-mL volumetric flask. The mixture was then diluted in Milli-Q water and mixed gently. Final concentrations of the dye and phosphate were 1 μM (0.38 mg/L for fluorescein and 0.48 mg/L for rhodamine 6G and rhodamine B) and 0.2 mM (19 mg-PO_4^{3-}/L), respectively. The linearity of fluorescence intensities in these dye concentrations was confirmed (see figure S1 in supplementary data). The test solutions were incubated at room temperature under dark conditions for 1 h. The pH of the solutions was maintained after the incubation. The fluorescence and absorption spectra were measured using a fluorescence spectrophotometer (F-2700; Hitachi High-Technologies Corporation, Tokyo, Japan) and UV-Vis spectrophotometer (UV-1800; Shimadzu Corporation, Kyoto, Japan), respectively. Both the excitation and fluorescence slit widths were 5.0 nm. All experiments were performed in triplicate.

For the inner filter effect, measured fluorescence spectra were corrected. When DHS absorbed the excitation and emission light, the measured fluorescence spectra were corrected by equation 1 (Lakowicz, 2006):

$$F_{corr} = F_{obs}\, antilog\left(\frac{A_{ex} + A_{em}}{2}\right), \quad (1)$$

where F_{corr} and F_{obs} are the corrected and observed fluorescence intensity, respectively, and A_{ex} and A_{em} are the absorbance of the test solution at excitation and emission

wavelengths, respectively.

The apparent fluorescence quantum yields were obtained by comparing the area under the observed fluorescence spectrum of the test solution with that of the solution of fluorescein in 0.1 M NaOH or rhodamine 6G in ethanol, which have a reported fluorescence quantum yield (Φ_R) of 0.91 and 0.95, respectively (Valeur and Berberan-Santos, 2012). The fluorescence quantum yield (Φ_S) for each test solution was calculated using equation 2 (Lakowicz, 2006):

$$\Phi_S = \Phi_R \times \frac{S_S}{S_R} \times \frac{A_R}{A_S} \times \left(\frac{\eta_S}{\eta_R}\right)^2, \quad (2)$$

where Φ is the quantum yield, S is the integrated area of the corresponding fluorescence spectrum, A is the absorbance at the excitation wavelength, η is the refractive index of the solvent used, and S and R refer to the sample and the reference fluorescent dyes, respectively.

2.3 Binding analysis

We analyzed the binding interaction of fluorescent dyes and DHS using equation 3 and 7. The Stern–Volmer equation is expressed as (Gauthier et al., 1986):

$$\frac{F_0}{F} = 1 + K_{doc}[DOC], \quad (3)$$

where F_0 and F are the fluorescence intensity of the fluorescent dye in the absence (F_0) and presence (F) of DHS, respectively, and K_{doc} is the binding coefficient. Plotting F_0/F against the DHS concentration ([DOC]) revealed a linear relationship between these values with an intercept of 1 and a slope that represents the value of K_{doc}. Pan et al. (2007) demonstrated the limitations of the Stern-Volmer plot for obtaining the binding coefficients between phenanthrene and DOM because the binding coefficients can vary with the concentrations of free phenanthrene as well as different DOM concentrations. Other studies reported non-linear binding interactions between PAHs and DOM and their binding coefficients depends on free solute concentration (Laor and Rebhun, 2002; Borisover et al., 2006). Laor et al. (2002) suggested the Freundlich-type equation to explain the non-linear binding. Considering these limitations, we evaluated the binding coefficients of two dyes with humic and fulvic acid under same experimental condition in which the total dye concentrations were 1 μM and the range of DHS concentrations were 0 – 5 mg-C/L. These DOC concentrations were used considering natural river water in Japan. If non-linear binding is expected, equation 4 is applied:

$$C_S = K_F {C_{free}}^n, \quad (4)$$

where C_S is the DHS-bound fluorescent dye concentration (w/w), C_{free} is the free dye

169 concentration (w/v), and K_F is the Freundlich coefficient. Equation 4 can be expressed

170 as:

$$C_S = \frac{C_{bound}}{[DOC]} = \frac{C_{total} - C_{free}}{[DOC]} = K_F {C_{free}}^n , \quad (5)$$

171 where C_{bound} and C_{total} are the bound and total dye concentrations (w/v), respectively.

172 Equation 5 can be rearranged as:

$$\frac{C_{total}}{C_{free}} = 1 + K_F[DOC]{C_{free}}^{n-1} \quad . (6)$$

173 The fluorescent intensity of a dye is proportional to its free concentration. Therefore,

174 equation 6 can be rearranged as follows:

$$\frac{F_0}{F} = 1 + {K_F}'[DOC]F^{n-1} . \quad (7).$$

175 We calculated the values of K_F' and n and obtained a non-linear model by Origin Pro

176 9.1J software. K_F' was modified to K_F by a factor of f^{n-1}. The f value is the specific

177 fluorescence activity of a fluorescent dye, which was given by fluorescence intensity

178 divided by its concentration.

179

180 **3. Results and discussion**

181 Figure 2 shows the absorption spectra of fluorescein and rhodamine 6G in the presence

182 of humic acid or fulvic acid. Fluorescein and rhodamine 6G exhibited strong absorption

183 bands with large molar absorption coefficients around 489 nm ($\varepsilon = 5.3 \times 10^4$ L mol^{-1}

184 cm^{-1}) and 526 nm ($\varepsilon = 8.5 \times 10^4$ L mol^{-1} cm^{-1}), respectively. In the wavelength region
185 below 450 nm, absorbance gradually increased with increasing DOC concentrations due
186 to chromogenic dissolved organic matter (CDOM; Zhang et al., 2009). Interestingly, the
187 absorption peak of rhodamine 6G at 526 nm shifted significantly to 536 nm upon
188 addition of humic acid (Fig. 2-(c)). This peak shift indicates that the mechanism of
189 binding interaction between rhodamine 6G and humic acid is different from that of
190 fluorescein-DHS complexes and rhodamine 6G-fulvic acid complex.
191
192 The fluorescence spectra of fluorescein and rhodamine 6G in the presence of humic acid
193 or fulvic acid are shown in Fig. 3. The inner filter effect correction factors were around
194 1.1 for all test solutions (data not shown). This value indicated that the inner filter
195 effects of DHS were negligible because the excitation and emission bands of DHS did
196 not overlap with those of fluorescent dyes (Henderson et al., 2009), and we prepared the
197 test solutions of the dyes with the absorbance under 0.1. As shown in Fig. 3, fluorescein
198 and rhodamine 6G produced sharp fluorescence bands with high fluorescence quantum
199 yields around 512 nm ($\Phi = 0.82$) and 551 nm ($\Phi = 0.86$), respectively. Fluorescence
200 quenching was observed with increasing DHS concentrations, with the fluorescence of
201 rhodamine 6G strongly decreasing upon addition of humic acid (Fig. 3-(c)). Apparent

fluorescence quantum yields of fluorescein and rhodamine 6G in the presence of humic acid or fulvic acid (5 mg-C/L) are listed in Table 1. Fluorescence quantum yields also decreased in response to the addition of DHS. Among them, the quantum yield of rhodamine 6G decreased significantly from 0.86 to 0.10 in response to the addition of humic acid. These results also indicate a strong fluorescence quenching effect of humic acid on rhodamine 6G.

The Stern–Volmer plots of the fluorescent dyes are shown in Fig. 4. Linear relationships were observed for fluorescein with humic and fulvic acids and rhodamine 6G with fulvic acid. The K_{doc} values are summarized in Table 2. The K_{doc} value of rhodamine 6G with fulvic acid (1.34×10^{-1} L/mg-C) is slightly larger than that of fluorescein with humic and fulvic acids (7.57×10^{-2} L/mg-C and 1.00×10^{-1} L/mg-C, respectively). Conversely, a non-linear curved plot towards the y-axis was obtained for rhodamine 6G with humic acid. Different concentration of rhodamine 6G also resulted in the non-linearity (see figure S2 in supplementary data). Some studies have attributed the non-linear binding to different causes. For example, combination of static and dynamic quenching could result in the non-linear plot (Pan et al., 2007). Another study also attributed the non-linear Stern-Volmer plot to the inherent heterogeneity of DOM (Laor

220 and Rebhun, 2002). We tried to evaluate the Stern-Volmer constant (K_{SV}) and the
221 stability constant (K_S) by using the equation considering static and dynamic quenching.
222 However, we could not get those values from the equation (see figure S3 in
223 supplementary data). Therefore, we concluded that static quenching was the primary
224 mechanism and we applied the Freundlich-type equation to explain the non-linear
225 binding. Previous researchers also often excluded dynamic quenching. The Freundlich
226 coefficient (K_F) of rhodamine 6G with humic acid was 7.84×10^{-1} L/mg-C and the n
227 value was 0.67. This strong quenching of rhodamine 6G with humic acid may indicate
228 the electrostatic interaction between cationic rhodamine 6G and anionic groups of
229 humic acid. Furthermore, this interaction could be strengthened by the hydrophobic
230 repulsion of less polar moieties from aqueous bulk. As compared with fulvic acid, the
231 increased interaction between rhodamine 6G and humic acid is in well agreement with
232 the significance of less hydrated hydrophobic moieties in its components.
233
234 Rhodamine B was also used for fluorescence quenching experiments with DHS. Figure
235 5 shows the Stern–Volmer plot of rhodamine B with DHS. The K_{doc} values for humic
236 and fulvic acids were 4.11×10^{-2} L/mg-C and 1.12×10^{-2} L/mg-C, respectively.
237 Interestingly, the non-linear binding was observed for rhodamine 6G but not for

238 rhodamine B. As compared with rhodamine 6G, rhodamine B has carboxylic group. The
239 carboxylic group was supposed to be ionized under the experimental pH condition and
240 the presence of ionized carboxylic group resulted in a greater aqueous solubility of the
241 dye as well as in an enhanced electrostatic rejection from DHS. In addition, the fact that
242 rhodamine B does not donate H-bond from its diethyl amino groups may also reduce the
243 binding affinity to DHS compared with rhodamine 6G.
244
245 **4. Conclusions**
246
247 In this study, the binding interactions between oppositely charged fluorescent dyes
248 (fluorescein and rhodamine 6G) and DHS (dissolved humic and fulvic acid) were
249 investigated by the fluorescence quenching method. The fluorescent intensities of dyes
250 decreased in response to the addition of DHS, and the binding coefficients were
251 obtained from the Stern–Volmer plots. Among them, the fluorescence of rhodamine 6G
252 was strongly quenched by humic acid and the non-linear Stern–Volmer plot was
253 obtained. This strong quenching may be caused by the electrostatic interaction between
254 cationic rhodamine 6G and anionic groups of humic acid. Then, the interaction could be
255 strengthened by the hydrophobic repulsion of less polar moieties from aqueous bulk. As

compared with rhodamine 6G, the quenching effects and binding coefficients of fluorescein with dissolved humic substances were relatively weak. These results would contribute to the practice of selecting suitable fluorescent dye tracers in aquatic and hydrology studies.

Acknowledgments

This research was supported by Grants-in-Aid for Scientific Research (KAKENHI Grant Nos. 26889054 and 26289178) from the Japan Society for the Promotion of Science.

References

Alford, R., Simpson, H.M., Duberman, J., Hill, G.C., Ogawa, M., Regino, C., Kobayashi, H., Choyke, P.L., 2009. Toxicity of organic fluorophores used in molecular imaging: literature review. Molecular Imaging 8 (6), 341-354.

Basabe-Desmonts, L., Reinhoudt, D.N., Crego-Calama, M., 2007. Design of fluorescent materials for chemical sensing. Chemical Society Reviews 36 (6), 993-1017.

Behrens, H., Beims, U., Dieter, H., Dietze, G., Eikmann, T., Grummt, T., Hanisch, H., Henseling, H., Kass, W., Kerndorff, H., Leibundgut, C., Muller-Wegener, U.,

Ronnefahrt, I., Scharenberg, B., Schleyer, R., Schloz, W., Tilkes, F., 2001. Toxicological and ecotoxicological assessment of water tracers. Hydrogeology Journal 9 (3), 321-325.

Borisover, M., Laor, Y., Bukhanovsky, N., Saadi, I., 2006. Fluorescence-based evidence for adsorptive binding of pyrene to effluent dissolved organic matter. Chemosphere 65 (11), 1925-1934.

Chen, X.Q., Pradhan, T., Wang, F., Kim, J.S., Yoon, J., 2012. Fluorescent chemosensors based on spiroring-opening of xanthenes and related derivatives. Chemical Reviews 112 (3), 1910-1956.

Gauthier, T.D., Shane, E.C., Guerin, W.F., Seitz, W.R., Grant, C.L., 1986. Fluorescence quenching method for determining equilibrium-constants for polycyclic aromatic-hydrocarbons binding to dissolved humic materials. Environmental Science & Technology 20 (11), 1162-1166.

Goppert, N., Goldscheider, N., 2008. Solute and colloid transport in karst conduits under low- and high-flow conditions. Ground Water 46 (1), 61-68.

Harden, H.S., Roeder, E., Hooks, M., Chanton, J.P., 2008. Evaluation of onsite sewage treatment and disposal systems in shallow karst terrain. Water Research 42 (10–11), 2585-2597.

292 Henderson, R.K., Baker, A., Murphy, K.R., Hamblya, A., Stuetz, R.M., Khan, S.J., 2009.
293 Fluorescence as a potential monitoring tool for recycled water systems: a review.
294 Water Research 43 (4), 863-881.
295 Hesketh, N., Jones, M.N., Tipping, E., 1996. The interaction of some pesticides and
296 herbicides with humic substances. Analytica Chimica Acta 327 (3), 191-201.
297 Jones, E.H., Smith, C.C., 2005. Non-equilibrium partitioning tracer transport in porous
298 media: 2-D physical modelling and imaging using a partitioning fluorescent dye.
299 Water Research 39 (20), 5099-5111.
300 Kwak, R., Guan, G.F., Peng, W.K., Han, J.Y., 2013. Microscale electrodialysis:
301 concentration profiling and vortex visualization. Desalination 308, 138-146.
302 Lakowicz, J.R., 2006. Principles of fluorescence spectroscopy, third ed. pp54-56 and
303 Springer, New York.
304 Laor, Y., Rebhun, M., 2002. Evidence for nonlinear binding of PAHs to dissolved humic
305 acids. Environmental Science & Technology 36 (5), 955-961.
306 Larsen, L.G., Crimaldi, J.P., 2006. The effect of photobleaching on PLIF. Experiments
307 in Fluids 41 (5), 803-812.
308 Li, Z.Y., Psaltis, D., 2008. Optofluidic dye lasers. Microfluidics and Nanofluidics 4
309 (1–2), 145-158.

310 Oba, Y., Poulson, S.R., 2012. Octanol-water partition coefficients (K-ow) vs. pH for
311 fluorescent dye tracers (fluorescein, eosin Y), and implications for hydrologic tracer
312 tests. Geochemical Journal 46 (6), 517-520.
313 Pan, B., Ghosh, S., Xing, B.S., 2007. Nonideal binding between dissolved humic acids
314 and polyaromatic hydrocarbons. Environmental Science & Technology 41 (18),
315 6472-6478.
316 Raber, B., Kogel-Knabner, I., Stein, C., Klem, D., 1998. Partitioning of polycyclic
317 aromatic hydrocarbons to dissolved organic matter from different soils.
318 Chemosphere 36 (1), 79-97.
319 Ravacha, C., Rebhun, M., 1992. Binding of organic solutes to dissolved humic
320 substances and its effects on adsorption and transport in the aquatic environment.
321 Water Research 26 (12), 1645-1654.
322 Sabaliunas, D., Webb, S.F., Hauk, A., Jacob, M., Eckhoff, W.S., 2003. Environmental
323 fate of Triclosan in the River Aire Basin, UK. Water Research 37 (13), 3145-3154.
324 Saini, G.S.S., Sharma, A., Kaur, S., Bindra, K.S., Sathe, V., Tripathi, S.K., Mhahajan,
325 C.G., 2009. Rhodamine 6G interaction with solvents studied by vibrational
326 spectroscopy and density functional theory. Journal of Molecular Structure 931
327 (1–3), 10-19.

328 Schlautman, M.A., Morgan, J.J., 1993. Effects of aqueous chemistry on the binding of
329 polycyclic aromatic-hydrocarbons by dissolved humic materials. Environmental
330 Science & Technology 27 (5), 961-969.
331 Smart, P.L., Laidlaw, M.S., 1977. An evaluation of some fluorescent dyes for water
332 tracing. Water Resources Research 13, 15-33.
333 Spark, K.M., Swift, R.S., 2002. Effect of soil composition and dissolved organic matter
334 on pesticide sorption. Science of the Total Environment 298 (1–3), 147-161.
335 Valeur, B., Berberan-Santos. M.N., 2012. Molecular fluorescence: principles and
336 applications, second ed. p272, Wiley-VCH, Weinheim.
337 Yamamoto, H., Liljestrand, H.M., Shimizu, Y., Morita, M., 2003. Effects of
338 physical-chemical characteristics on the sorption of selected endocrine disruptors by
339 dissolved organic matter surrogates. Environmental Science & Technology 37 (12),
340 2646-2657.
341 Yuan, L., Lin, W.Y., Zheng, K.B., He, L.W., Huang, W.M., 2013. Far-red to near
342 infrared analyte-responsive fluorescent probes based on organic fluorophore
343 platforms for fluorescence imaging. Chemical Society Reviews 42 (2), 622-661.
344 Zhang, Y.L., van Dijk, M.A., Liu, M.L., Zhu, G.W., Qin, B.Q., 2009. The contribution
345 of phytoplankton degradation to chromophoric dissolved organic matter (CDOM) in

346 eutrophic shallow lakes: field and experimental evidence. Water Research 43 (18),
347 4685-4697.
348
349

Figure and table captions

Fig. 1 Chemical structures of fluorescein, rhodamine 6G, and rhodamine B.

Fig. 2 Absorption spectra of fluorescein (a, b) and rhodamine 6G (c, d) with increasing DOC concentrations of humic acid or fulvic acid. The spectra were taken at DOC concentrations of 0, 0.5, 1, 2, and 5 mg-C/L. The concentration of the fluorescent dye was 1.0 μM (0.38 mg/L for fluorescein and 0.48 mg/L for rhodamine 6G).

Fig. 3 Fluorescence spectra of fluorescein (a, b) and rhodamine 6G (c, d) with increasing DOC concentrations of humic acid or fulvic acid. The spectra were taken at DOC concentrations of 0, 0.5, 1, 2, and 5 mg-C/L. The concentration of the fluorescent dye was 1.0 μM (0.38 mg/L for fluorescein and 0.48 mg/L for rhodamine 6G). The excitation wavelengths of fluorescein and rhodamine 6G were 480 nm and 520 nm, respectively.

Fig. 4 Stern-Volmer plots for fluorescein (a) and rhodamine 6G (b) with increasing DOC concentrations of humic acid or fulvic acid. Fluorescence intensities of fluorescein

368 and rhodamine 6G were plotted at 512 nm and 551 nm, respectively. Solid lines
369 represent linear relationships. A non-linear relationship is shown as a dashed line.
370
371 Fig. 5 Stern–Volmer plots for rhodamine B with increasing DOC concentrations of
372 humic acid or fulvic acid. Fluorescence intensities of rhodamine B were plotted at 574
373 nm.
374
375 Table 1 Apparent fluorescent quantum yields of fluorescein and rhodamine 6G in the
376 presence of DHS (5 mg-C/L).
377
378 Table 2 K_{doc}, Intercept, K_F, n, and r^2 value obtained in this study.
379

1 Table 1 Apparent fluorescent quantum yields of fluorescein and rhodamine 6G in the

2 presence of DHS (5 mg-C/L).

3

Fluorescent dye	DHS	Φ
Fluorescein	–	0.82 ± 0.01
	Humic acid	0.45 ± 0.02
	Fulvic acid	0.55 ± 0.02
Rhodamine 6G	–	0.86 ± 0.01
	Humic acid	0.10 ± 0.00
	Fulvic acid	0.58 ± 0.02

Table 2 K_{doc}, Intercept, K_F, n, and r^2 value obtained in this study.

Fluorescent dye	DHS	K_{doc} (L/mg-C) (= Slope)	Intercept	K_F (L/mg-C)	n	r^2
Fluorescein	Humic acid	7.57×10^{-2} ($\pm 1.60 \times 10^{-3}$)	1.01 ($\pm 3.41 \times 10^{-2}$)	–	–	0.992
	Fulvic acid	1.00×10^{-1} ($\pm 9.90 \times 10^{-3}$)	1.00 ($\pm 2.29 \times 10^{-2}$)	–	–	0.994
Rhodamine 6G	Humic acid	–	–	7.84×10^{-1} ($\pm 1.92 \times 10^{-1}$)	0.67 ($\pm$0.090)	0.999
	Fulvic acid	1.34×10^{-1} ($\pm 3.78 \times 10^{-2}$)	1.02 ($\pm 2.08 \times 10^{-2}$)	–	–	0.998

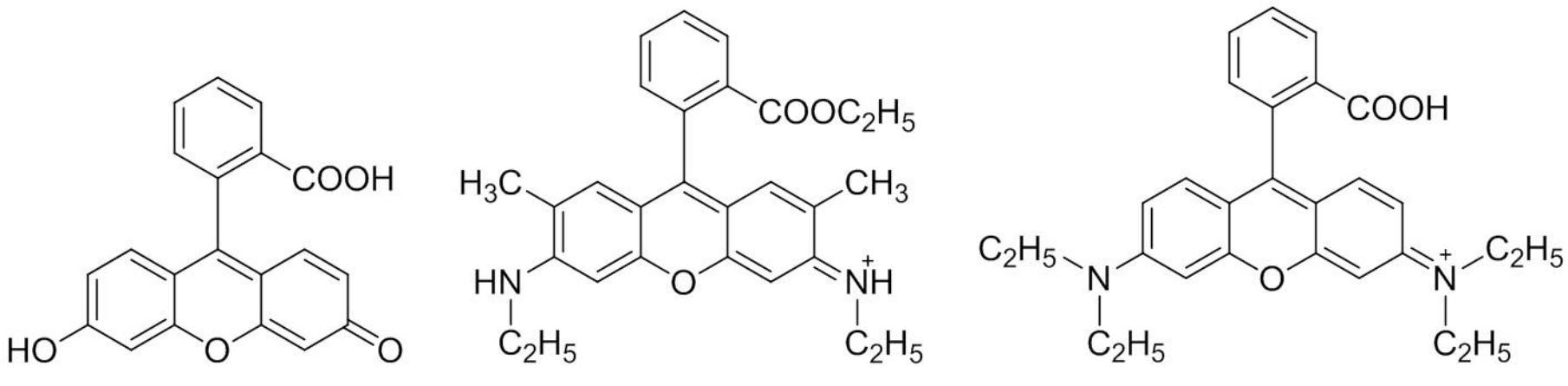

Fig. 1 Chemical structures of fluorescein, rhodamine 6G, and rhodamine B.

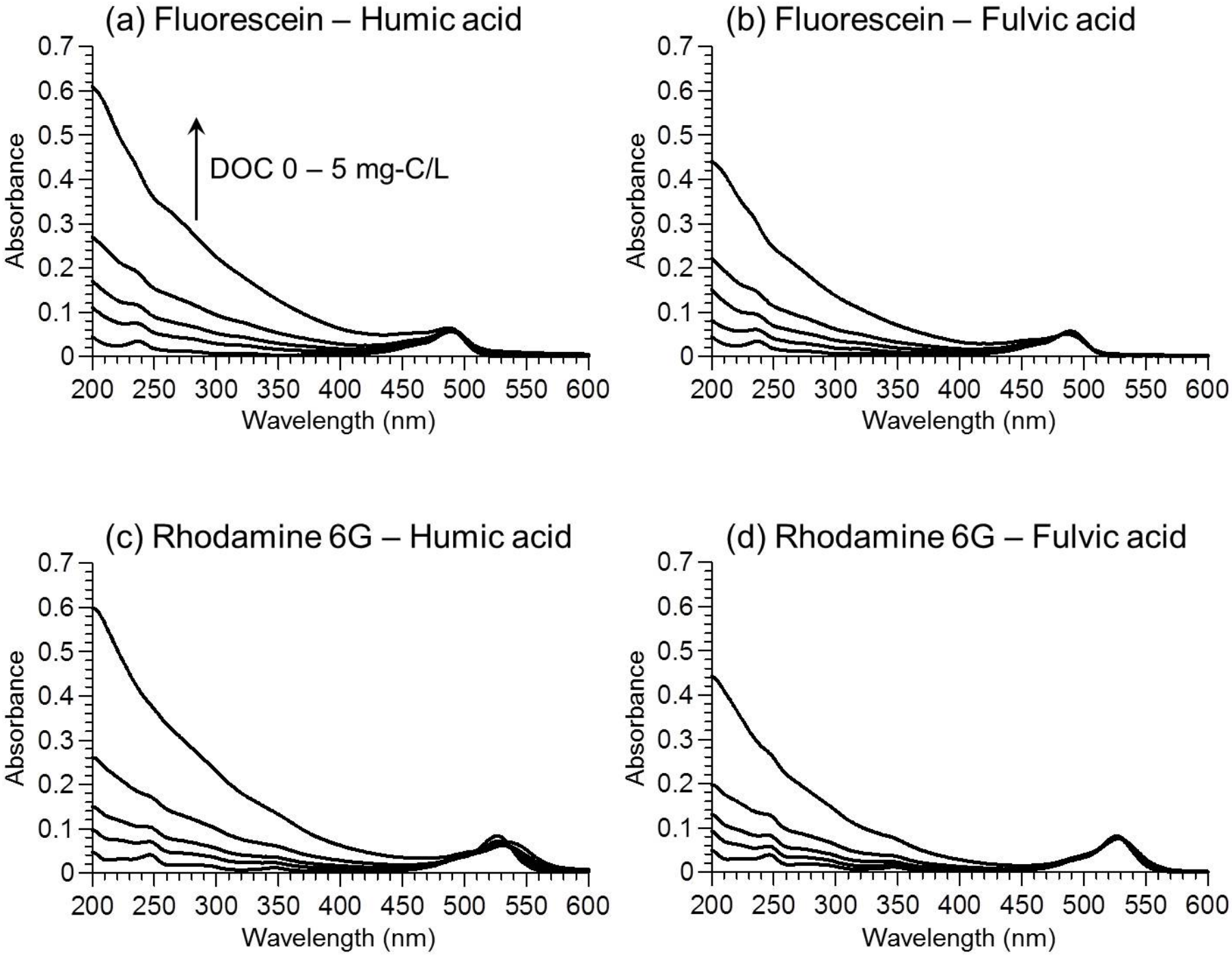

Fig. 2 Absorption spectra of fluorescein (a, b) and rhodamine 6G (c, d) with increasing DOC concentrations of humic acid or fulvic acid. The spectra were taken at DOC concentrations of 0, 0.5, 1, 2, and 5 mg-C/L. The concentration of the fluorescent dye was 1.0 μM (0.38 mg/L for fluorescein and 0.48 mg/L for rhodamine 6G).

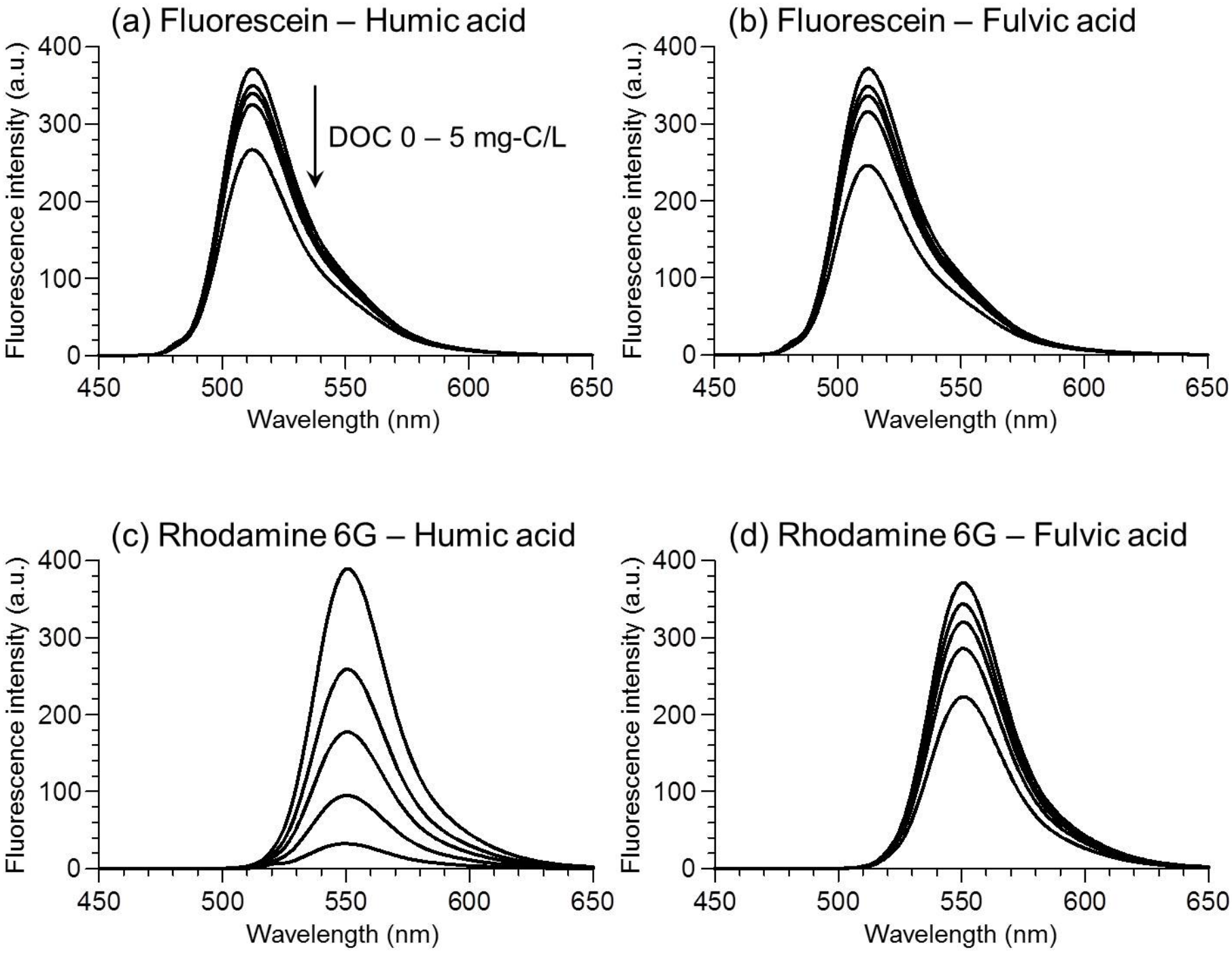

Fig. 3 Fluorescence spectra of fluorescein (a, b) and rhodamine 6G (c, d) with increasing DOC concentrations of humic acid or fulvic acid. The spectra were taken at DOC concentrations of 0, 0.5, 1, 2, and 5 mg-C/L. The concentration of the fluorescent dye was 1.0 μM (0.38 mg/L for fluorescein and 0.48 mg/L for rhodamine 6G). The excitation wavelengths of fluorescein and rhodamine 6G were 480 nm and 520 nm, respectively.

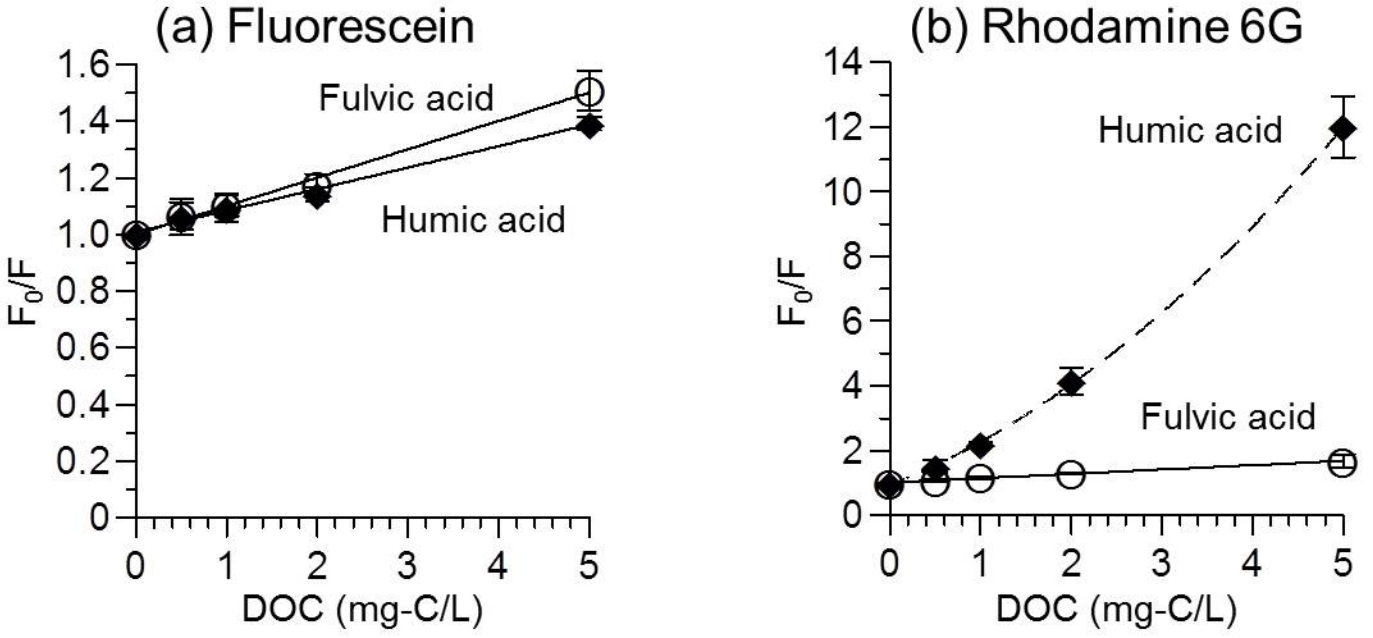

Fig. 4 Stern-Volmer plots for fluorescein (a) and rhodamine 6G (b) with increasing DOC concentrations of humic acid or fulvic acid. Fluorescence intensities of fluorescein and rhodamine 6G were plotted at 512 nm and 551 nm, respectively. Solid lines represent linear relationships. A non-linear relationship is shown as a dashed line.

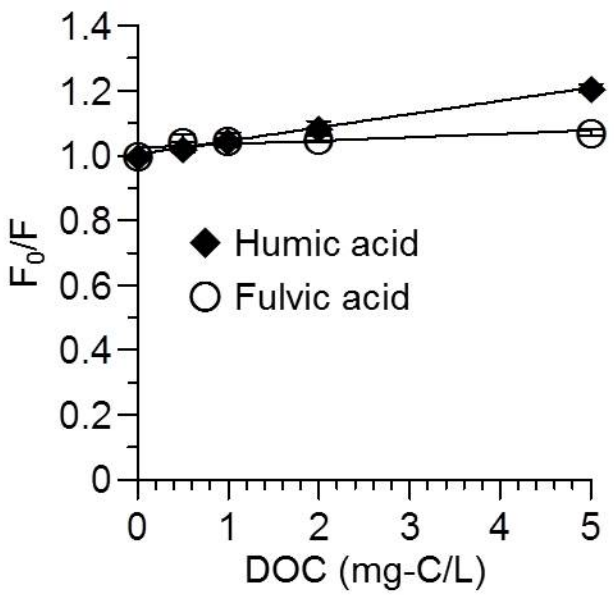

Fig. 5 Stern–Volmer plots for rhodamine B with increasing DOC concentrations of humic acid or fulvic acid. Fluorescence intensities of rhodamine B were plotted at 574 nm.